Jurnal Ilmiah Teknik Elektro Komputer dan Informatika (JITEKI)
Vol. 10, No. 4, December 2024, pp. 858-869
ISSN: 2338-3070, DOI: 10.26555/jiteki.v10i4.30327

Enhancing DenseNet Accuracy in Retinal Disease Classification with Contrast Limited Adaptive Histogram Equalization

Galih Restu Baihaqi[1], Shafatyra Reditha Shalsadilla[1], Afifulail Maya Nur Maulidiya[2], Lailil Muflikhah[1]
[1]Faculty of Computer Science, Brawijaya University, Malang, Indonesia
[2]Faculty of Medical, Brawijaya University, Malang, Indonesia

ARTICLE INFO

Article history:

Received November 16, 2024
Revised December 30, 2024
Accepted January 11, 2025

Keywords:

CLAHE;
Classification;
DenseNet;
Retina

ABSTRACT

Retinal diseases are serious conditions that can cause vision impairment and, in severe cases, blindness, affecting 6.3% to 17.9% of cases per 100,000 people annually worldwide. Early diagnosis is crucial but often time-consuming, prompting the use of Artificial Intelligence (AI) models like DenseNet, part of the Convolutional Neural Network (CNN) architecture, to streamline the process. This study utilizes the Retinal OCT Images dataset from Kaggle, comprising 83,600 images categorized into four classes. To address the low contrast in Optical Coherence Tomography (OCT) images, the Contrast Limited Adaptive Histogram Equalization (CLAHE) technique was applied during preprocessing. Results indicate that DenseNet without CLAHE achieved an accuracy, precision, recall, and F1-score of 95%, while incorporating CLAHE improved these metrics to 98%. The application of CLAHE also reduced classification bias and error, enhancing model reliability despite requiring more training epochs (43 compared to 39 without CLAHE). These findings demonstrate the potential of CLAHE to optimize DenseNet performance in retinal disease classification. Future research could explore other image enhancement techniques or apply the method to different retinal disease datasets, contributing to improved diagnostic accuracy in clinical settings.

This work is licensed under a Creative Commons Attribution-Share Alike 4.0

Corresponding Author:

Lailil Muflikhah, Brawijaya University, Indonesia
Email: lailil@ub.ac.id

1. INTRODUCTION

The retina is a light-sensitive layer at the back of the eye that functions as part of the visual system by receiving light stimuli and transmitting them to the brain, where they are processed into images [1]. Worldwide, the prevalence of retinal diseases is substantial and is expected to increase over time. One study projects the number of diabetic retinopathy (DR) cases to rise from 103 million in 2020 to over 160 million by 2045, with the most significant increases anticipated in Africa and the Middle East [2]. Furthermore, the global prevalence of DR has reached 27%, with the highest rates also occurring in Africa and the Middle East [3]. Concerning other retinal diseases, another study [4] reported that retinal vein occlusion (RVO) affected over 28 million people in 2015, making it the second most common retinal vascular disorder after DR. In Nepal, a study [5] found that retinal diseases were present in 52.4% of elderly participants, with age-related macular degeneration being the most common condition. These findings highlight the urgent need to enhance global attention to retinal diseases and the importance of early detection initiatives. Despite these concerns, manual diagnostic methods are still predominant, which are often labor-intensive and prone to variability, creating a significant research gap.

Despite advances in diagnostic tools, retinal disease diagnosis remains challenging due to the high variability in image quality and the time-consuming manual processes required. Existing diagnostic methods often struggle with handling the wide contrast variation and image noise present in Optical Coherence

Tomography (OCT) scans. These challenges create a research gap in improving image preprocessing techniques and developing models capable of achieving high diagnostic accuracy efficiently. Enhancing the preprocessing of retinal images is crucial to enable deep learning models to reliably extract features and improve classification outcomes [6]. Recently, technological advancements, particularly in Artificial Intelligence (AI), have accelerated significantly, especially in Convolutional Neural Networks (CNN), which is a part of Deep Learning [7]-[17]. CNN has made substantial contributions in analyzing medical images [18]-[24]. Densely Connected Convolutional Networks (DenseNet) is a CNN architecture designed to leverage inter-layer connectivity more effectively, thus providing better performance in image classification [25]. In this study, the DenseNet architecture was chosen to process retinal image data due to its advantages in generating rich and efficient feature representations. DenseNet facilitates better information transfer from the initial layer to the final layer through dense connections between layers so that each layer receives richer and more detailed feature information. This is crucial for improving accuracy in abnormality detection in medical images, including diabetic retinopathy in retinal images. By connecting each layer directly to all previous layers, DenseNet can capture fine details important in medical analysis, which are often difficult to detect with traditional convolutional architectures [26]. DenseNet also overcomes the vanishing gradient problem, which allows the gradient flow to remain stable despite the high depth of the network. This results in more effective and deep model training, allowing DenseNet to recognize complex patterns in retinal images with higher accuracy. For OCT image classification, DenseNet has demonstrated its effectiveness in previous studies with high levels of accuracy and reliability [27], [28].

However, a common issue encountered in retinal image classification is the wide range of contrast variations in images obtained from medical devices, such as Optical Coherence Tomography (OCT) [29]. The contrast variation in OCT images can result from differences in lighting conditions during image capture. Additionally, the clarity of the lens and the quality of the OCT device itself can affect the image quality and diversity. This issue can pose challenges for Deep Learning models in recognizing important retinal features [30]. Therefore, improving image quality to enhance contrast is necessary so that the resulting features are more relevant and easier for the DenseNet model to extract.

Contrast Limited Adaptive Histogram Equalization (CLAHE) is an effective image processing technique for enhancing local contrast in medical images. CLAHE works by limiting contrast enhancement to avoid noise amplification [31]. CLAHE divides an image into regions and performs histogram equalization on each region with adjusted contrast limitations, thus achieving more uniform and detailed contrast enhancement that is highly beneficial for creating quality features in retinal images [32]-[34]. In a study of MRI data such as Alzheimer's, CLAHE was shown to improve image contrast very well and can improve the accuracy of CNN models. Other studies mention that CLAHE can improve the quality of MRI medical images by sharpening image features and contrast, which proves that CLAHE is better than the Median Filtering technique. For retinal images, CLAHE ensures that critical details such as blood vessels and lesion boundaries are more visible, aiding in improved feature extraction.

Overall, this study applies CLAHE to address contrast variation challenges in OCT images, aiming to enhance DenseNet's performance in retinal disease classification. By integrating CLAHE, this study contributes to advancing diagnostic accuracy and facilitating early retinal disease detection for better eye health outcomes. Additionally, the study addresses critical challenges in the manual diagnosis process and provides a scalable solution for automated retinal disease diagnosis.

2. LITERATURE REVIEW

2.1. Retina

The retina is a crucial layer in the eye that plays an essential role in the visual process. Its function is to capture light entering the eye, which is then converted into signals sent to the brain to be processed and interpreted into images or visuals. The retina is highly susceptible to various diseases, which can impact the quality of vision and, ultimately, lead to blindness. Some retinal diseases include Choroidal Neovascularization (CNV), Diabetic Macular Edema (DME), and Drusen, which may be caused by age-related factors, other conditions like diabetes, and genetic factors. These diseases can result in blurred vision [35]-[38]. To capture retinal images, a medical device known as Optical Coherence Tomography (OCT) is used [39], [40], and a description of each disease is shown in Fig. 1.

2.2. DenseNet

The Densely Connected Convolutional Network (DenseNet) is a CNN architecture designed to enhance feature utilization while reducing the number of required parameters. Unlike traditional CNNs, which connect

layers sequentially, DenseNet employs dense connections where each layer receives input from all preceding layers and transmits its output to all subsequent layers. This connectivity allows DenseNet to better maintain model structure and prevents the loss of gradient flow, which commonly occurs in very deep Deep Learning models [41], [42]. A block diagram of DenseNet is shown in Fig. 2.

Fig. 1. Retinal Diseases Captured Using OCT

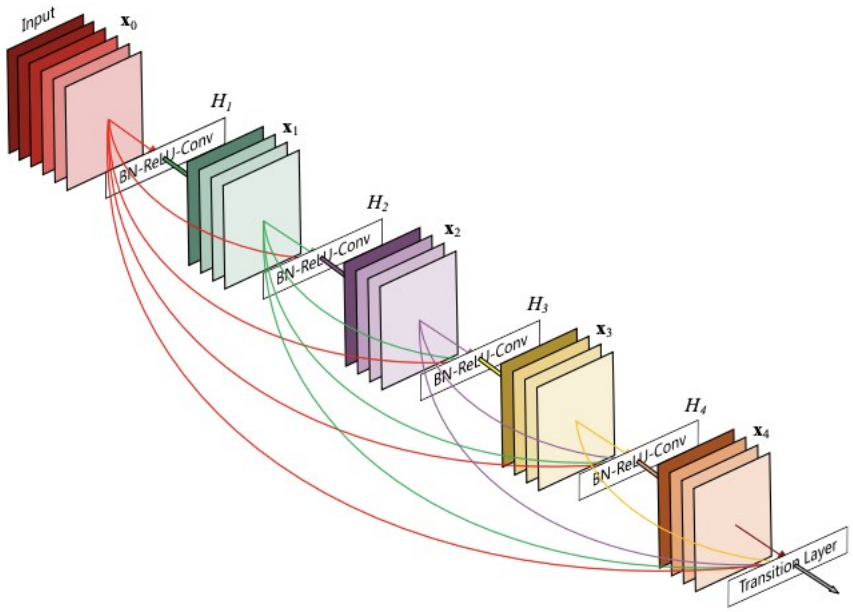

Fig. 2. Block Diagram of DenseNet

2.3. CLAHE

Contrast Limited Adaptive Histogram Equalization (CLAHE) is a contrast enhancement method that applies spatial domain techniques to achieve uniform contrast improvement across an image while considering maximum entropy and effectively limiting contrast. This technique is well-suited for enhancing contrast in relatively low-contrast medical images [43]-[45]. The formula used to calculate the gray level in CLAHE is shown in (3), and the gray-level value distribution technique can be measured using (1) and (2).

$$g = [g_{max} - g_{min}] \times P(f) + g_{min} \tag{1}$$

$$g = g_{min} - \left(\frac{1}{a}\right) \times \ln [1 - P(f)] \tag{2}$$

$$y = P\big(f(x|b)\big) = \int_0^x \frac{x}{b^2} e^{-\frac{x^2}{2b^2}} \tag{3}$$

Remark g is pixel value, g_{max} is maximum pixel value, g_{min} is minimum pixel value, $P(f)$ is CPD (Cumulative Probability Distribution), a is clip parameters, y is cumulative probability value/Rayleigh, b is scale parameters for the Rayleigh distribution.

2.4. Confusion Matrix

The Confusion Matrix is a technique commonly used to evaluate the classification results produced by AI models, whether they are Machine Learning or Deep Learning models. The Confusion Matrix is useful for showing the accuracy of a model that has been trained on training data and subsequently evaluated using prepared testing data [46], [47]. The Confusion Matrix consists of TP, TN, FP, and FN, as shown in Fig. 3. TP is True Positive, TN is True Negative, FP is False Positive, FN is False Negative.

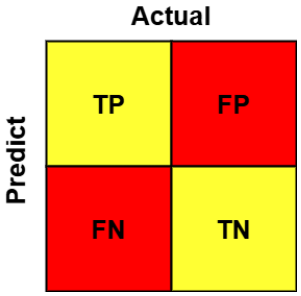

Fig. 3. Confusion Matrix

3. METHOD

3.1. Dataset

The dataset used is obtained from Kaggle under the name "Retinal OCT Images (optical coherence tomography)," which consists of 4 classes: CNV, DME, Drusen, and Normal. The total dataset comprises 83,600 images captured using an OCT device. The dataset is imbalanced, with the majority class being CNV, accounting for 44.5% (37,216 images). Meanwhile, the other classes, such as Normal, DME, and Drusen, represent 31.5% (26,344 images), 13.7% (11,420 images), and 10.3% (8,620 images), respectively. The data distribution in the dataset is shown in Fig. 4, and sample images for each class are displayed in Fig. 5.

The images in the dataset were captured using OCT devices, which can produce high-resolution cross-sectional images of the retina. However, variations in lighting conditions, device calibration, and patient eye movement during image capture might result in image quality inconsistencies. These inconsistencies can introduce variability in the dataset, which may affect model performance [48], [49].

Fig. 4. Dataset Distribution per Class

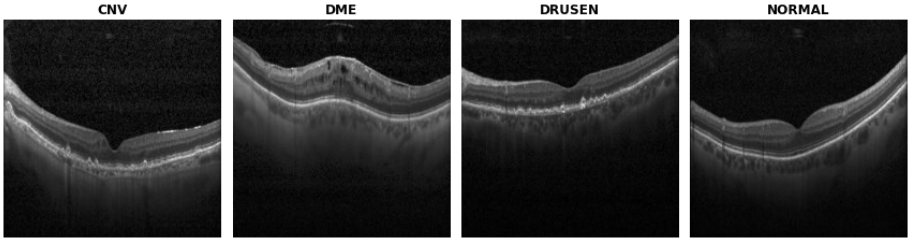

Fig. 5. Example Dataset per Class

3.2. Data Preprocessing

Data preprocessing is a technique used to prepare the data before it is processed by the model. First, the preprocessing technique used is Down Sampling, which is applied to handle the class imbalance in the dataset by reducing the dominance of the majority class. Next, the CLAHE technique is applied to enhance the contrast of the dataset, improving feature visibility in OCT images. The dataset is then resized to a standard size of 224x224 pixels, which is commonly used in CNNs like DenseNet to ensure consistent input dimensions [50]-[52]. Finally, the dataset is split into three parts: training data (80%), validation data (10%), and testing data (10%) to train, monitor, and evaluate the model respectively. The flow of data preprocessing is shown in Fig. 6.

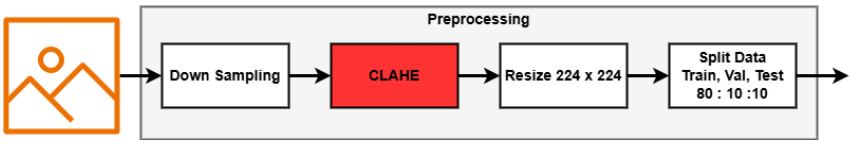

Fig. 6. Data Preprocessing Block Diagram

3.3. System Block Diagram

The classification system was built using the DenseNet121 model. The system workflow starts with image data input, followed by data preprocessing. Once data preprocessing is complete, the model is trained using the training data, with validation data monitoring the training process. During the training process, the epochs used were 50. However, the epoch used to perform classification was based on the epoch that obtained the highest accuracy on the validation data. The learning rate used was 0.001. Once the model has been successfully trained, it is evaluated using a confusion matrix. This process is illustrated in Fig. 7.

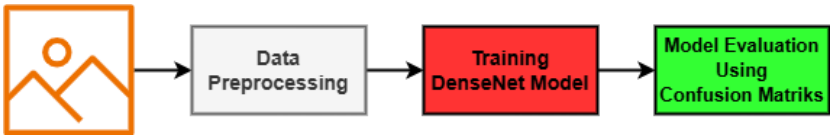

Fig. 7. System Block Diagram

3.4. Testing Scenario

To test the effect of CLAHE on improving the accuracy of the DenseNet model in classifying retinal images, an experiment is conducted by comparing the DenseNet model's performance without CLAHE transformation on the images with the DenseNet model applied to images that have been transformed using CLAHE. These two processes are illustrated in Fig. 8.

In Fig. 8, the process is divided into 4 parts. The main difference lies in the preprocessing stage, where one dataset undergoes CLAHE transformation, and the other does not. After the preprocessing stage, both datasets continue the same training process, using the DenseNet121 model with 50 epochs, a learning rate of 0.001, and a batch size of 64. After the training process, the classification process uses the best epoch based on the accuracy on the validation data obtained during the training process. After each training process is complete, an evaluation is performed to measure the performance of the trained model using testing data. The outputs generated for both models include Accuracy, Precision, Recall, and F1-Score values.

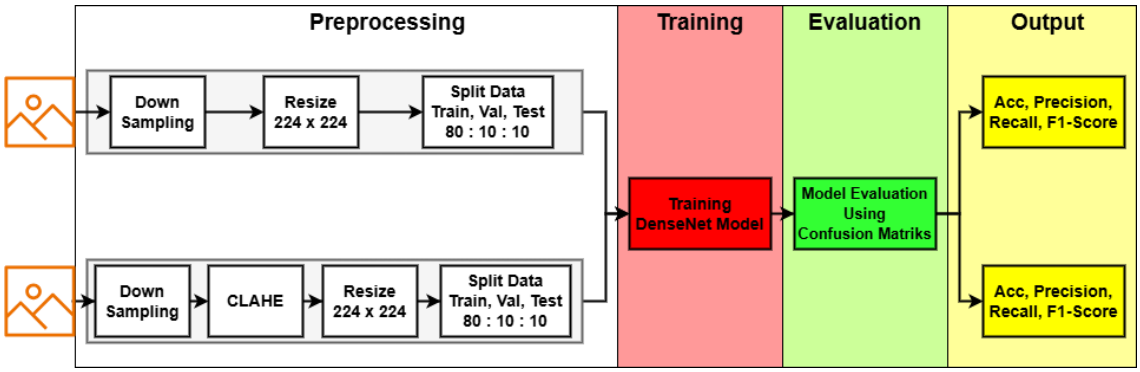

Fig. 8. Testing Scenario Block Diagram

3.5. Model Evaluation

The values from the confusion matrix can be used to calculate and evaluate the classification model built. Model evaluation is measured based on accuracy, precision, recall, and F1-score. The equations used to calculate accuracy, precision, recall, and F1-score are shown in (4)–(7).

$$Accuracy = \frac{TP + TN}{TP + TN + FP + FN} \tag{4}$$

$$Precision = \frac{TP}{TP + FP} \tag{5}$$

$$Recall = \frac{TP}{TP + FN} \tag{6}$$

$$F1 - Score = 2 \times \frac{Precison \times Recall}{Precision + Recall} \tag{7}$$

Equations (4)–(7) represent the parameter indicators used to measure the model's performance. Accuracy is an evaluation metric that measures the percentage of correct predictions out of the total predictions made by the model. Precision measures the model's accuracy in predicting the positive class. Recall measures how well the model detects the actual positive class. The F1-score is the harmonic mean of precision and recall.

4. RESULT AND DISCUSSION

4.1. Image Transformation using CLAHE

Contrast Limited Adaptive Histogram Equalization (CLAHE) is an effective technique for enhancing local contrast in images, especially for low-contrast data such as retinal OCT images. The application of CLAHE significantly improves the visibility of details in retinal structures, which is critical for accurate disease detection and classification. The results of the image transformation before and after applying CLAHE for the four classes CNV, DME, Drusen, and Normal are presented in Fig. 9.

As seen in Fig. 9, the transformation enhances the local contrast of the images. For example, in the CNV class, features such as abnormal tissue and fluid accumulations are more distinct, making pathological changes easier to identify. Similarly, in the DME class, the subtle fluid-filled areas within the retinal layers become more prominent after applying CLAHE. In the Drusen class, the deposits beneath the retina are better visualized, while in the Normal class, the retinal layers appear sharper and more clearly defined. This enhancement ensures that critical features are not obscured by low contrast, thus reducing the likelihood of misclassification.

The enhancement process in CLAHE operates by dividing each image into smaller, non-overlapping regions (tiles) and performing histogram equalization locally within each tile. A clip limit is applied to avoid over-amplification of noise, ensuring that the transformation focuses on meaningful contrast enhancement. This localized approach is particularly advantageous for retinal OCT images, where different regions may have varying levels of contrast.

To quantitatively evaluate the enhancement, the Peak Signal-to-Noise Ratio (PSNR) of the images after CLAHE transformation was measured, yielding a value of 28.55. This metric indicates a significant improvement in image quality, as a higher PSNR reflects better fidelity and reduced distortion in the transformed images. The PSNR value further validates that CLAHE effectively enhances image contrast without introducing excessive noise or artifacts.

In summary, CLAHE transformation enhances the visibility of subtle abnormalities in retinal structures, which is crucial for disease classification. By improving local contrast, achieving a PSNR of 28.55, and ensuring uniform enhancement across the image, CLAHE prepares the data for further analysis and ensures that the input images are informative and suitable for robust classification tasks.

4.2. Down Sampling

In Fig. 4, the dataset exhibits an imbalanced distribution, with the majority class (CNV) having a significantly higher number of data points compared to the minority class (Drusen). To address this imbalance, down sampling was performed to ensure an equal number of data points across all classes. This approach minimizes the risk of model overfitting to the majority class by providing a balanced representation of the dataset. The minority class, Drusen, contains 8,620 data points, and thus, the other classes CNV, Normal, and

DME were limited to the same number of data points. Consequently, the total dataset size after down sampling was reduced to 34,480 data points. The dataset distribution after down sampling is presented in Fig. 10.

Down sampling was chosen in this study as it avoids potential biases that may arise from oversampling or up sampling techniques, which could artificially replicate or generate synthetic data points. Additionally, the choice of down sampling was made based on the sufficient dataset size even after down sampling, ensuring that the reduced dataset still provided ample data points for robust training and evaluation. This technique also aligns with the computational constraints of the study, ensuring efficient processing without compromising data quality.

Following the down sampling process, the dataset was divided into training, validation, and testing sets using an 80:10:10 ratio. This resulted in 27,584 data points for training, and 3,448 data points each for validation and testing. The choice of an 80:10:10 split balances the need for a substantial amount of training data while maintaining enough validation and testing data to monitor and evaluate model performance. This split ratio ensures a reliable evaluation of the model's generalization capability while avoiding potential overfitting.

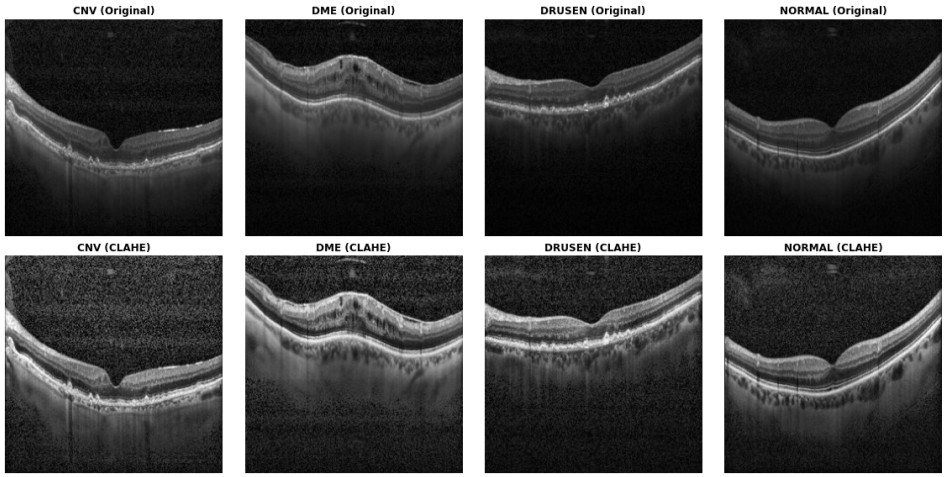

Fig. 9. Results of Image Transformation Using CLAHE

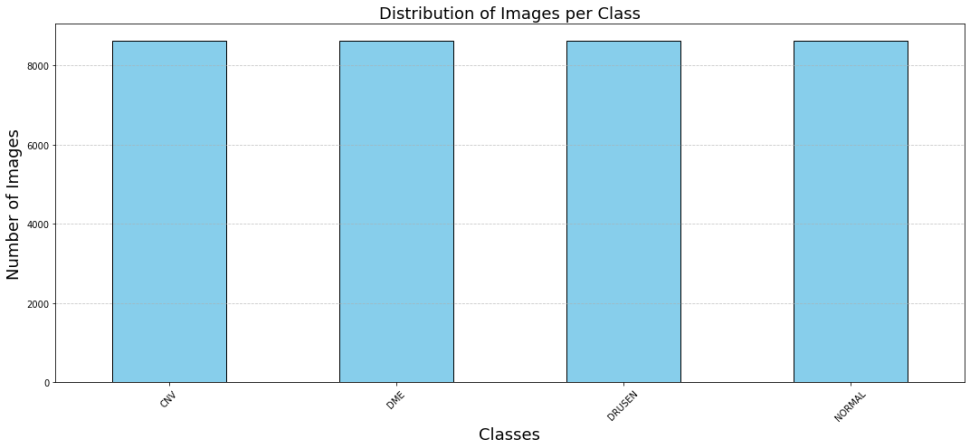

Fig. 10. Dataset Distribution per Class After Downsampling

4.3. Model Evaluation Results

4.3.1. DenseNet Model Without CLAHE

Images without CLAHE have low contrast, as shown in Fig. 9. During the training process, the best epoch based on training accuracy is achieved at epoch 39, as shown in Fig. 11(a). Fig. 11(b) displays the confusion matrix, which indicates that the model achieved the best predictions in the Normal class with 843 correct predictions. Meanwhile, the model's worst predictions were in the Drusen class, with 793 correct predictions. The accuracy achieved by this model is 95%.

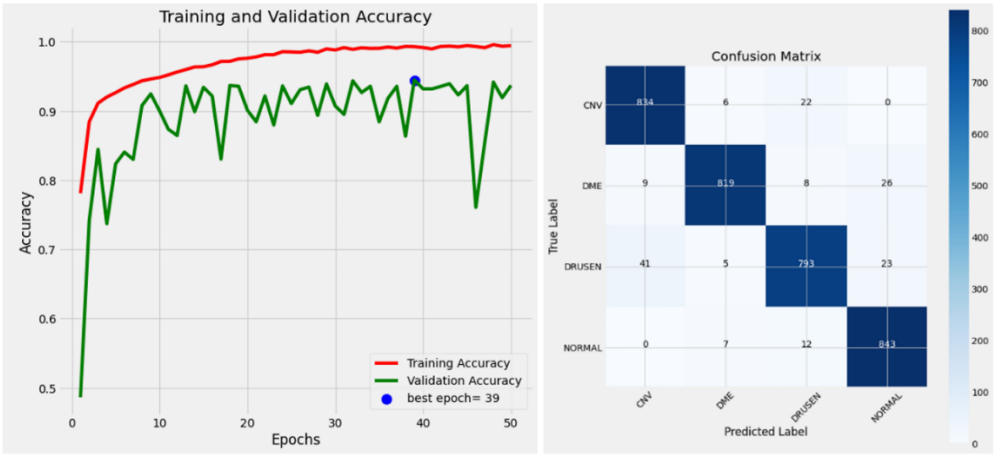

Fig. 11. (a) Training Process, (b) Confusion Matrix Results of DenseNet Model Without CLAHE

4.3.2. DenseNet Model With CLAHE

CLAHE images are those with enhanced contrast, as shown in Fig. 9. During the training process, the best epoch based on training accuracy is achieved at epoch 43, as shown in Fig. 12(a). Fig. 12(b) displays the confusion matrix, which indicates that the model achieved the best predictions in the Normal class with 850 correct predictions. Meanwhile, the model's worst predictions were in the CNV class, with 831 correct predictions. The accuracy achieved by this model is 98%.

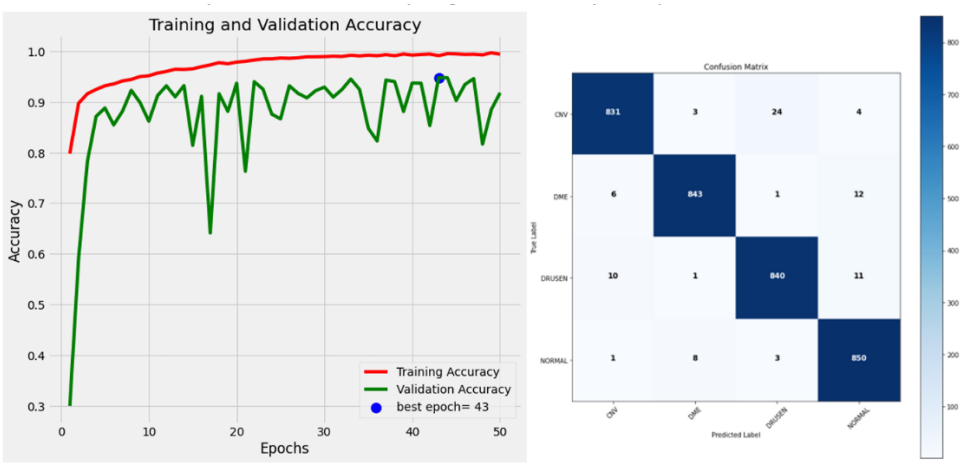

Fig. 12. (a) Training Process, (b) Confusion Matrix Results of DenseNet Model With CLAHE

4.4. Overall Evaluation

From the test results, it can be seen that the DenseNet model without CLAHE reached its best epoch faster, in the 39th epoch. Compared to the DenseNet model using CLAHE, the model reached its best epoch at the 43rd epoch. However, determining the best model is not only based on the best epoch, but also considers the highest accuracy, precision, recall, and F1-score metrics. Based on this analysis, the DenseNet model with CLAHE shows better performance. In addition to DenseNet, the implementation of CLAHE also improved the accuracy of the ResNet model by 2%, indicating that CLAHE contributed positively to improving the accuracy of the model applied to Optical Coherence Tomography (OCT) images. However, for other common CNN models, there was no significant increase in accuracy due to the implementation of CLAHE.

Overall, from the entire set of tests conducted, the DenseNet model with CLAHE produced the best performance compared to other models, such as standard CNN and ResNet, as presented in Table 1. This confirms that the use of CLAHE in OCT image preprocessing can improve the classification quality of the DenseNet model, while demonstrating the relevance of this strategy in improving the performance of certain models.

Table. 1. Comparison of Model Evaluation Results

Model Name	Accuracy (%)	Precision (%)	Recall (%)	F1-Score (%)
CNN Base	77	77	77	77
CNN Base + CLAHE	77	77	77	77
ResNet	92	92	92	92
ResNet + CLAHE	94	94	94	94
DenseNet	95	95	95	95
DenseNet + CLAHE	**98**	**98**	**98**	**98**

5. CONCLUSION

This study demonstrates the effectiveness of integrating Contrast Limited Adaptive Histogram Equalization (CLAHE) into the preprocessing stage of retinal Optical Coherence Tomography (OCT) images for enhancing the performance of deep learning models, particularly DenseNet. Retinal diseases pose significant risks of vision impairment and blindness, necessitating accurate and efficient diagnostic tools. By addressing the challenge of low contrast in OCT images through CLAHE, this study achieved significant improvements in classification accuracy.

The DenseNet model without CLAHE achieved accuracy, precision, recall, and F1-score values of 95%, with the best epoch reached at epoch 39. After incorporating CLAHE, these metrics improved to 98%, with the best epoch occurring at epoch 43. This improvement highlights the ability of CLAHE to enhance local contrast, making subtle features in retinal structures more discernible and reducing the likelihood of misclassification. The higher performance of the DenseNet model with CLAHE confirms its suitability for retinal disease classification tasks, as it consistently outperformed baseline CNN and ResNet models, with CLAHE contributing an additional accuracy improvement of 2% to the ResNet model.

Despite these promising results, certain limitations must be acknowledged. This study primarily focused on DenseNet and CLAHE, leaving room to explore other advanced architectures and image enhancement techniques. Additionally, while CLAHE was effective in this context, its impact on other medical imaging modalities or datasets requires further investigation. Future work could explore the scalability of this approach with larger datasets, test its applicability in real-time clinical settings, and incorporate statistical analyses, such as confidence intervals or standard deviations, to provide deeper insights into model robustness.

In conclusion, the integration of CLAHE in the preprocessing stage significantly enhances the performance of deep learning models for retinal disease classification. This finding emphasizes the importance of tailored preprocessing techniques in medical image analysis and sets the foundation for further advancements in automated retinal diagnostics, benefiting healthcare providers, patients, and researchers in achieving early and accurate diagnosis of retinal diseases.

REFERENCES

[1] M.-J. Lee and G. Zeck, "Electrical imaging of light-induced signals across and within retinal layers," *Front Neurosci*, vol. 14, 2020, https://doi.org/10.3389/fnins.2020.563964.

[2] Z. Teo *et al.*, "Global prevalence of diabetic retinopathy and projection of burden through 2045: systematic review and meta-analysis," *Ophthalmology*, vol. 128, no. 11, pp. 1580-1591, 2021, https://doi.org/10.1016/j.ophtha.2021.04.027.

[3] R. Thomas, S. Halim, S. Gurudas, S. Sivaprasad, and D. Owens, "IDF Diabetes Atlas: A review of studies utilising retinal photography on the global prevalence of diabetes related retinopathy between 2015 and 2018," *Diabetes Res Clin Pract*, vol. 107840, 2019, https://doi.org/10.1016/j.diabres.2019.107840.

[4] P. Song, Y. Xu, M. Zha, Y. Zhang, and I. Rudan, "Global epidemiology of retinal vein occlusion: a systematic review and meta-analysis of prevalence, incidence, and risk factors," *J Glob Health*, vol. 9, 2019, https://doi.org/10.7189/jogh.09.010427.

[5] R. Thapa, S. Khanal, H. Tan, S. Thapa, and G. Rens, "Prevalence, pattern and risk factors of retinal diseases among an elderly population in Nepal: the Bhaktapur Retina Study," *Clin Ophthalmol*, vol. 14, pp. 2109–2118, 2020, https://doi.org/10.2147/OPTH.S262131.

[6] R. T. Yanagihara, C. S. Lee, D. S. W. Ting, and A. Y. Lee, "Methodological Challenges of Deep Learning in Optical Coherence Tomography for Retinal Diseases: A Review," *Transl Vis Sci Technol*, vol. 9, no. 2, p. 11, 2020, https://doi.org/10.1167/tvst.9.2.11.

[7] A. Nilla and E. B. Setiawan, "Film recommendation system using content-based filtering and convolutional neural network (CNN) classification methods," *Jurnal Ilmiah Teknik Elektro Komputer dan Informatika (JITEKI)*, vol. 10, no. 1, pp. 17–29, 2024, https://doi.org/10.26555/jiteki.v9i4.28113.

[8] W. Riyadi and Jasmir, "Comparative analysis of optimizer effectiveness in GRU and CNN-GRU models for airport traffic prediction," *Jurnal Ilmiah Teknik Elektro Komputer dan Informatika (JITEKI)*, vol. 10, no. 3, pp. 580–593, 2024, https://doi.org/10.26555/jiteki.v10i3.29659.

[9] M. Krichen, "Convolutional neural networks: A survey," *Computers*, vol. 12, p. 151, 2023, https://doi.org/10.3390/computers12080151.
[10] Y.-F. Qin, H. Bao, F. Wang, J. Chen, Y. Li, and X. Miao, "Recent progress on memristive convolutional neural networks for edge intelligence," *Advanced Intelligent Systems*, vol. 2, 2020, https://doi.org/10.1002/aisy.202000114.
[11] W. Xu, J. He, Y. Shu, and H. Zheng, "Advances in convolutional neural networks," *IntechOpen*, pp. 1-22, 2020, https://doi.org/10.5772/intechopen.93512.
[12] L. Alzubaidi *et al.*, "Review of deep learning: Concepts, CNN architectures, challenges, applications, future directions," *J Big Data*, vol. 8, 2021, https://doi.org/10.1186/s40537-021-00444-8.
[13] H. Li, "Computer network connection enhancement optimization algorithm based on convolutional neural network," in *Proc. International Conference on Networking, Communications and Information Technology (NetCIT)*, 2021, pp. 281–284. https://doi.org/10.1109/NetCIT54147.2021.00063.
[14] N. Babbar, A. Kumar, and V. K. Verma, "Predicting wheat yield using sequential and deep convolutional neural networks," in *Proc. 5th International Conference on Electronics and Sustainable Communication Systems (ICESC)*, pp. 1104–1108, 2024, https://doi.org/10.1109/ICESC60852.2024.10689887.
[15] G. Kumar, P. Kumar, and D. Kumar, "Brain tumor detection using convolutional neural network," in *Proc. IEEE International Conference on Mobile Networks and Wireless Communications (ICMNWC)*, 2021, pp. 1–6. https://doi.org/10.1109/ICMNWC52512.2021.9688460.
[16] J. J. Zhou, "Research on the complexity characteristics of convolutional neural networks," in *Proc. IEEE 7th Information Technology and Mechatronics Engineering Conference (ITOEC)*, pp. 402–405, 2023, https://doi.org/10.1109/ITOEC57671.2023.10291768.
[17] N. Yamsani, M. B. Jabar, M. M. Adnan, A. H. A. Hussein, and S. Chakraborty, "Facial emotional recognition using faster regional convolutional neural network with VGG16 feature extraction model," in *Proc. 3rd International Conference on Mobile Networks and Wireless Communications (ICMNWC)*, pp. 1–6, 2023, https://doi.org/10.1109/ICMNWC60182.2023.10435819.
[18] T. Zhou, X. Ye, H. Lu, X. Zheng, S. Qiu, and Y. Liu, "Dense Convolutional Network and Its Application in Medical Image Analysis," *Biomed Res Int*, p. 2384830, 2022, https://doi.org/10.1155/2022/2384830.
[19] L. Khriji, S. Bouaafia, S. Messaoud, A. Ammari, and M. Machhout, "Secure convolutional neural network-based Internet-of-healthcare applications," *IEEE Access*, vol. 11, pp. 36787–36804, 2023, https://doi.org/10.1109/ACCESS.2023.3266586.
[20] Z. Li, F. Liu, W. Yang, S. Peng, and J. Zhou, "A survey of convolutional neural networks: Analysis, applications, and prospects," *IEEE Trans Neural Netw Learn Syst*, vol. 33, pp. 6999–7019, 2020, https://doi.org/10.1109/TNNLS.2021.3084827.
[21] H. Yu, L. Yang, Q. Zhang, D. Armstrong, and M. Deen, "Convolutional neural networks for medical image analysis: State-of-the-art, comparisons, improvement, and perspectives," *Neurocomputing*, vol. 444, pp. 92–110, 2021, https://doi.org/10.1016/J.NEUCOM.2020.04.157.
[22] P. Bir and V. Balas, "A review on medical image analysis with convolutional neural networks," in *IEEE International Conference on Computing, Power and Communication Technologies (GUCON)*, pp. 870–876, 2020, https://doi.org/10.1109/GUCON48875.2020.9231203.
[23] G. Kourounis, A. Elmahmudi, B. Thomson, J. Hunter, H. Ugail, and C. Wilson, "Computer image analysis with artificial intelligence: A practical introduction to convolutional neural networks for medical professionals," *Postgrad Med J*, vol. 99, pp. 1287–1294, 2023, https://doi.org/10.1093/postmj/qgad095.
[24] G. R. Baihaqi, S. R. Shalsadilla, and M. K. Argaputri, "Enhancing ResNet with Ghost Weight Normalization For Improved Retina Disease Classification," *IC-ITECHS*, vol. 5, no. 1, 2024, https://doi.org/10.32664/ic-itechs.v5i1.1554.
[25] C. Mohanty *et al.*, "Using Deep Learning Architectures for Detection and Classification of Diabetic Retinopathy," *Sensors (Switzerland)*, vol. 23, 2023, https://doi.org/10.3390/s23125726.
[26] Z. Ma, Q. Xie, P. Xie, F. Fan, X. Gao, and J. Zhu, "HCTNet: A Hybrid ConvNet-Transformer Network for Retinal Optical Coherence Tomography Image Classification," *Biosensors (Basel)*, vol. 12, 2022, https://doi.org/10.3390/bios12070542.
[27] M. Deaconu, D. Popescu, and L. Ichim, "Automatic detection of blood vessels in retinal images using FC-DenseNet neural networks," in *Proc. 25th Int. Conf. Syst. Theory, Control and Comput. (ICSTCC)*, pp. 449–454, 2021, https://doi.org/10.1109/ICSTCC52150.2021.9607051.
[28] S. A. P, S. Kar, G. S, V. Gopi, and P. Palanisamy, "OctNET: A Lightweight CNN for Retinal Disease Classification from Optical Coherence Tomography Images," *Comput Methods Programs Biomed*, p. 105877, 2020, https://doi.org/10.1016/j.cmpb.2020.105877.
[29] L. Chen, C. Tang, Z. H. Huang, M. Xu, and Z. Lei, "Contrast Enhancement and Speckle Suppression in OCT Images Based on a Selective Weighted Variational Enhancement Model and an SP-FOOPDE Algorithm," *Journal of the Optical Society of America A*, vol. 38, no. 7, pp. 973–984, 2021, https://doi.org/10.1364/JOSAA.422047.
[30] A. B and K. Kalirajan, "Contrast Enhancement of Alzheimer's MRI Using Histogram Analysis," *Journal of Innovative Image Processing*, vol. 5, no. 4, pp. 379-389, 2023, https://doi.org/10.36548/jiip.2023.4.003.
[31] B. Li, M. Qiu, Y. Ke, S. Zhu, and S. Luo, "Recognition algorithm of partial discharge pulse sequence based on CLAHE enhancement," in *Proc. 3rd Int. Conf. Inf. Technol. Electr. Eng.*, pp. 483-488, 2020, https://doi.org/10.1145/3452940.3453033.

[32] D. A. Anam, L. Novamizanti, and S. Rizal, "Classification of Retinal Pathology via OCT Images Using Convolutional Neural Network," in *International Conference on Computer System, Information Technology, and Electrical Engineering (COSITE)*, pp. 12–17, 2021, https://doi.org/10.1109/COSITE52651.2021.9649630.
[33] Y. Ren, Z. He, Y. Deng, and B. Huang, "Data augmentation for improving CNNs in medical image classification," in *Proc. 8th International Conference on Intelligent Computing and Signal Processing (ICSP)*, pp. 1174–1180, 2023, https://doi.org/10.1109/ICSP58490.2023.10248857.
[34] B. Vinoothna, "Design and development of contrast-limited adaptive histogram equalization technique for enhancing MRI images by improving PSNR, UIQI parameters in comparison with median filtering," *ECS Trans*, vol. 107, 2022, https://doi.org/10.1149/10701.14819ecst.
[35] R. Denandra, A. Fariza, and Y. R. Prayogi, "Eye Disease Classification Based on Fundus Images Using Convolutional Neural Network," *International Electronics Symposium (IES)*, pp. 563–568, 2023, https://doi.org/10.1109/IES59143.2023.10242558.
[36] F. Dhaoui and A. Zrelli, "Retinal Diseases Classification System Using OCT Images Combined with CNN Models," in *Proc. International Symposium on Networks, Computers and Communications (ISNCC)*, pp. 1–6, 2023, https://doi.org/10.1109/ISNCC58260.2023.10323745.
[37] J. Kim and L. Tran, "Retinal Disease Classification from OCT Images Using Deep Learning Algorithms," in *Proc. IEEE Conference on Computational Intelligence in Bioinformatics and Computational Biology (CIBCB)*, pp. 1–6. 2021, https://doi.org/10.1109/CIBCB49929.2021.9562919.
[38] G. R. Baihaqi, S. R. Shalsadilla, and M. K. Argaputri, "Accuracy Improvement of Convolutional Neural Network with Ghost Weight Normalization for Pneumonia Classification," *Jurnal Galaksi*, vol. 1, no. 3, pp. 143–152, Dec. 2024, https://doi.org/10.70103/galaksi.v1i3.35.
[39] M. R. Ibrahim, K. M. Fathalla, and S. M. Youssef, "HyCAD-OCT: A Hybrid Computer-Aided Diagnosis of Retinopathy by Optical Coherence Tomography Integrating Machine Learning and Feature Maps Localization," *Applied Sciences*, vol. 10, p. 4716, 2020, https://doi.org/10.3390/app10144716.
[40] Z. Ai *et al.*, "FN-OCT: Disease Detection Algorithm for Retinal Optical Coherence Tomography Based on a Fusion Network," *Front Neuroinform*, vol. 16, 2022, https://doi.org/10.3389/fninf.2022.876927.
[41] M. Bundea and G. M. Danciu, "Pneumonia Image Classification Using DenseNet Architecture," *Information*, vol. 15, no. 10, 2024, https://doi.org/10.3390/info15100611.
[42] Y. He, Y. Wu, and C. Wang, "Based on Hybrid Densenet-121 with Support Vector Machine Algorithm for Lettuce and Chili," in *2023 IEEE International Conference on Mechatronics and Automation (ICMA)*, pp. 1593–1597, 2023, https://doi.org/10.1109/ICMA57826.2023.10215571.
[43] B. B. Singh and S. Patel, "Efficient Medical Image Enhancement Using CLAHE Enhancement and Wavelet Fusion," *Int J Comput Appl*, vol. 167, no. 5, 2017, https://cir.nii.ac.jp/crid/1361418519958753920.
[44] Y. Zhang, X. Li, and Z. Wang, "Improved CLAHE algorithm based on independent component analysis," in *Proc. IEEE Int. Conf. Image Process. (ICIP)*, pp. 1234–1238, 2022, https://doi.org/10.1109/EIT63098.2024.10762100.
[45] S. Kumar and R. P. Singh, "A review on CLAHE based enhancement techniques," in *Proc. IEEE Conf. Comput. Intell. Commun. Technol. (CICT)*, pp. 1–6, 2022, https://doi.org/10.1109/IC3I59117.2023.10397722.
[46] I. Markoulidakis, I. Rallis, I. Georgoulas, G. Kopsiaftis, A. Doulamis, and N. Doulamis, "Multiclass Confusion Matrix Reduction Method and Its Application on Net Promoter Score Classification Problem," *Technologies (Basel)*, vol. 9, no. 4, 2021, https://doi.org/10.3390/technologies9040081.
[47] A. Arias-Duart, E. Mariotti, D. Garcia-Gasulla, J. M. Alonso-Moral, "A confusion matrix for evaluating feature attribution methods," *IEEE Trans Neural Netw Learn Syst*, vol. 33, no. 8, pp. 1234–1245, 2022, https://openaccess.thecvf.com/content/CVPR2023W/XAI4CV/html/Arias-Duart_A_Confusion_Matrix_for_Evaluating_Feature_Attribution_Methods_CVPRW_2023_paper.html'.
[48] J. Kugelman, D. Alonso-Caneiro, S. A. Read, S. J. Vincent, F. K. Chen, and M. J. Collins, "Effect of Altered OCT Image Quality on Deep Learning Boundary Segmentation," *IEEE Access*, vol. 8, pp. 43537–43553, 2020, https://doi.org/10.1109/ACCESS.2020.2977355.
[49] J. Wang, G. Deng, and W. Li, "Deep learning for quality assessment of retinal OCT images," *Biomed Opt Express*, vol. 10, no. 12, pp. 6057–6072, 2019, https://doi.org/10.1364/boe.10.006057.
[50] M. Abhishek, Y. Fu, and H. Zhang, "DenseNetx: Efficient DenseNets for Remote Scene Classification without Pretraining," in *IEEE Geoscience and Remote Sensing Letters*, pp. 1-6, 2023. https://doi.org/10.1109/LGRS.2023.10228170.
[51] W. Zhang, L. Yu, and Z. Liu, "DenseNeXt: An Efficient Backbone for Image Classification," *IEEE Access*, vol. 11, pp. 23456–23463, 2023, https://doi.org/10.1109/ACCESS.2023.10146197.
[52] X. Wang, Y. Li, and Z. Zhou, "Multiple Feature Reweight DenseNet for Image Classification," *IEEE Access*, vol. 6, pp. 61134–61141, 2019, https://doi.org/10.1109/ACCESS.2018.2879354.